NANO LETTERS

pubs.acs.org/NanoLett

Letter

Ultrafast Laser 3D Nanolithography of Fiber-Integrated Silica Microdevices

Dezhi Zhu,[▽] Shangben Jiang,[▽] Changrui Liao,* Lei Xu, Ying Wang, Dejun Liu, Weijia Bao, Famei Wang, Haoqiang Huang, Xiaoyu Weng, Liwei Liu, Junle Qu, and Yiping Wang

Cite This: *Nano Lett.* 2024, 24, 9734−9742

Read Online

ACCESS | Metrics & More | Article Recommendations | Supporting Information

ABSTRACT: Fiber-integrated micro/nanostructures play a crucial role in modern industry, mainly owing to their compact size, high sensitivity, and resistance to electromagnetic interference. However, the three-dimensional manufacturing of fiber-tip functional structures beyond organic polymers remains challenging. It is essential to construct fiber-integrated inorganic silica with designed functional nanostructures for microsystem applications. Here, we develop a strategy for the 3D nanolithography of fiber-integrated silica from hybrid organic−inorganic materials by ultrafast laser-induced multiphoton absorption. Without silica nanoparticles and polymer additives, the acrylate-functionalized precursors can be locally cross-linked through a nonlinear effect. Followed by annealing at low temperature, the as-printed micro/nanostructures are transformed to high-quality silica with sub-100 nm resolution. Silica microcantilever probes and microtoroid resonators are directly integrated onto the optical fiber, showing strong thermal stability and quality factors. This work provides a promising strategy for fabricating desired fiber-tip silica micro/nanostructures, which is helpful for the development of integrated functional device applications.

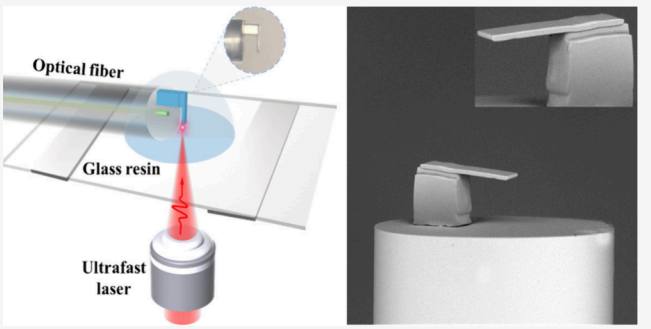

KEYWORDS: *ultrafast laser, multiphoton effect, 3D nanolithography, fiber-integrated silica*

With the development of "Lab on Fiber" technology, the integration of micro/nanofunctional structures on optical fiber tips has been widely applied in sensing and imaging due to their compact size, high sensitivity, and resistance to electromagnetic interference.[1−3] The optical fiber tip provides an inherently extensible platform, enabling interaction between the light and the integrated device. However, three-dimensional (3D) manufacturing of fiber-integrated functional structures beyond organic polymers, which are known to deform when exposed to harsh environments, remains challenging. This limitation significantly restricts the potential applications of fiber-integrated functional devices. Inorganic nanostructures with immense potential applications have garnered significant research interest from fundamental exploration and practical implementations.[4−8] Silica glass is a crucial inorganic material with diverse utility in scientific research, industry, and society. This is primarily attributed to its remarkable mechanical strength, exceptional optical transparency, and thermal and chemical resistance.[9−13] Various additive manufacturing techniques for fabricating silica glass have been investigated, including stereolithography,[14,15] digital light printing,[16] and two-photon polymerization (TPP).[17,18] While these methods have demonstrated the ability to create 3D silica glass structures, their capacity to achieve precise feature sizes is generally limited to several tens of micrometers and submicrometer resolution. Moreover, it is important to note that the requirement for high-temperature sintering hinders the application of these techniques, as they rely on silica nanoparticle-loaded composites. To eliminate the organic components and effectively bond the silica nanoparticles into cohesive structures, a sintering process spanning several days is imperative. This sintering is conducted under vacuum or in an inert atmosphere at temperatures as high as 1300 °C, which exceeds the melting points of optical fibers. Thus, traditional additive manufacturing strategies based on silica nanoparticle-loaded composites are generally unsuitable for on-fiber manufacturing.

3D printing of hybrid organic−inorganic materials represents a promising, nanoparticle-free alternative for fabricating inorganic nanostructures.[19] This strategy is under extensive investigation for the manufacture of micro/nanoceramics. By employing TPP printing and subsequent thermal decomposition with sol−gel precursors, it becomes possible to create

Received: June 7, 2024
Revised: July 19, 2024
Accepted: July 22, 2024
Published: July 24, 2024

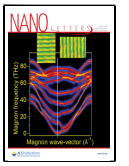

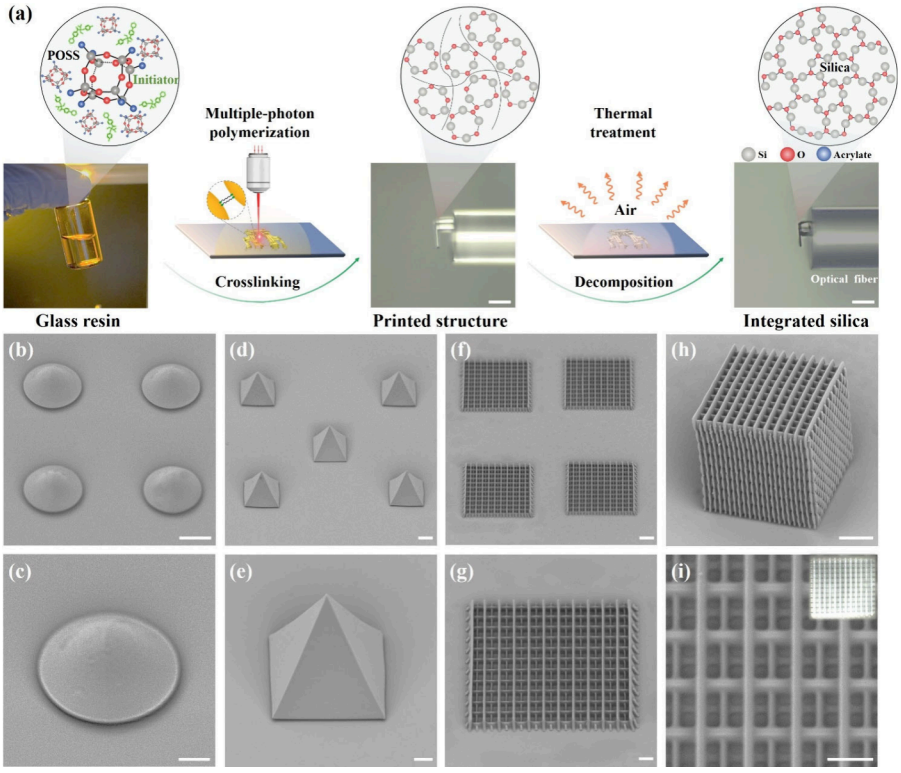

Figure 1. Ultrafast laser multiphoton 3D nanolithography of fiber-integrated functional silica glass. (a) Schematic of the printing and thermal treatment process of acrylate-functionalized POSS resin on the optical fiber tip. (b, c) Tilt-view SEM images of fabricated silica parabolic microlenses array. (d, e) Tilt-view SEM images of rectangular pyramid array. (f, g) Tilt-view SEM images of single-layer woodpile micro/nanostructure array. (h) Tilt-view SEM images of multilayer woodpile micro/nanostructures and (i) close-up top view of the nanostructures with inset optical micrograph. Scale bars: (a) 50 μm, (b, d, f, h) 10 μm, (c, e, g) 5 μm, and (i) 2 μm.

3D nanostructures with feature sizes as small as 200 nm in ceramics[20] and glassy carbon.[21] Compared to nanoparticle-loaded composites, the sol–gel strategies entail intricate preprint preparations and a high-temperature treatment of printed structures at 1100 °C for material densification.[22] Recently, polyhedral oligomeric silsesquioxanes (POSS) featuring silicon–oxygen frameworks have found successful applications in the printing of silica glass.[23] When using hydrogen silsesquioxanes as precursors, the hardened gel film state might impose printing constraints.[24,25] TPP of fused silica through a sinterless, low-temperature process was realized using POSS and acrylic oligomer composites.[26] Although silica glass with good mechanical and optical properties was manufactured, the direct fabrication of functional silica glass featuring nanometer-scale structures on the optical fiber tip remained unexplored. Thus, fiber-integrated silica devices with high resolution still require further development for micro-system application.[27]

In this study, we develop a strategy for the 3D fabrication of fiber-integrated silica glass based on ultrafast laser multiphoton nanolithography. The acrylate-functionalized POSS can be locally cross-linked through a nonlinear absorption process without silica nanoparticles and polymer additives. Followed by firing at low temperatures, the as-printed structures are transformed to high-quality silica with nanoscale resolution. It is demonstrated that ultrafast laser-fabricated silica microcantilevers and microtoroid resonators can be directly integrated on the optical fiber tip for optical microsystem applications, showing strong thermal stability and quality factors.

CONCEPT OF ULTRAFAST LASER 3D NANOLITHOGRAPHY OF FIBER-INTEGRATED FUNCTIONAL SILICA

Figure 1a schematically illustrates that the designed functional silica structures directly integrated on the optical fiber tip can be fabricated through ultrafast laser 3D nanolithography, followed by low-temperature thermal treatment in an air atmosphere. In contrast to conventional silica nanoparticle-loaded composites, the glass resin is a distinctive negative photoresist comprising two essential components: acrylate-functionalized POSS and a photoinitiator. The POSS cage,[28,29] serving as the source for silicon–oxygen frameworks, plays a vital role in silica conversion. Unlike sol–gel resins, acrylic functional groups,[30−32] enabling printing in a liquid state, are crucial for high-quality printing. The selected photoinitiator (Irgacure 369)[33] facilitated the polymerization of the acrylic groups upon exposure to an ultrafast laser, which possesses efficient nonlinear absorption and radical generation. The glass resin was prepared by mixing and heating the two above components, resulting in a stable and transparent liquid. Unlike in the previous work,[26] additional acrylic oligomers were not used in order to further reduce the structure shrinkage. Multiphoton 3D nanoprinting was performed using a 1030 nm wavelength femtosecond laser equipped with a home-built equipment.[34−37] The resin was dripped onto an optical fiber tip, and a laser beam was precisely focused into the resin. Within the confined focal region, the photoinitiator underwent multiphoton absorption, leading to chemical bond breaking and radical generation. These radicals initiated the cross-linking of the acrylic functional groups, resulting in the

https://doi.org/10.1021/acs.nanolett.4c02680
Nano Lett. 2024, 24, 9734−9742

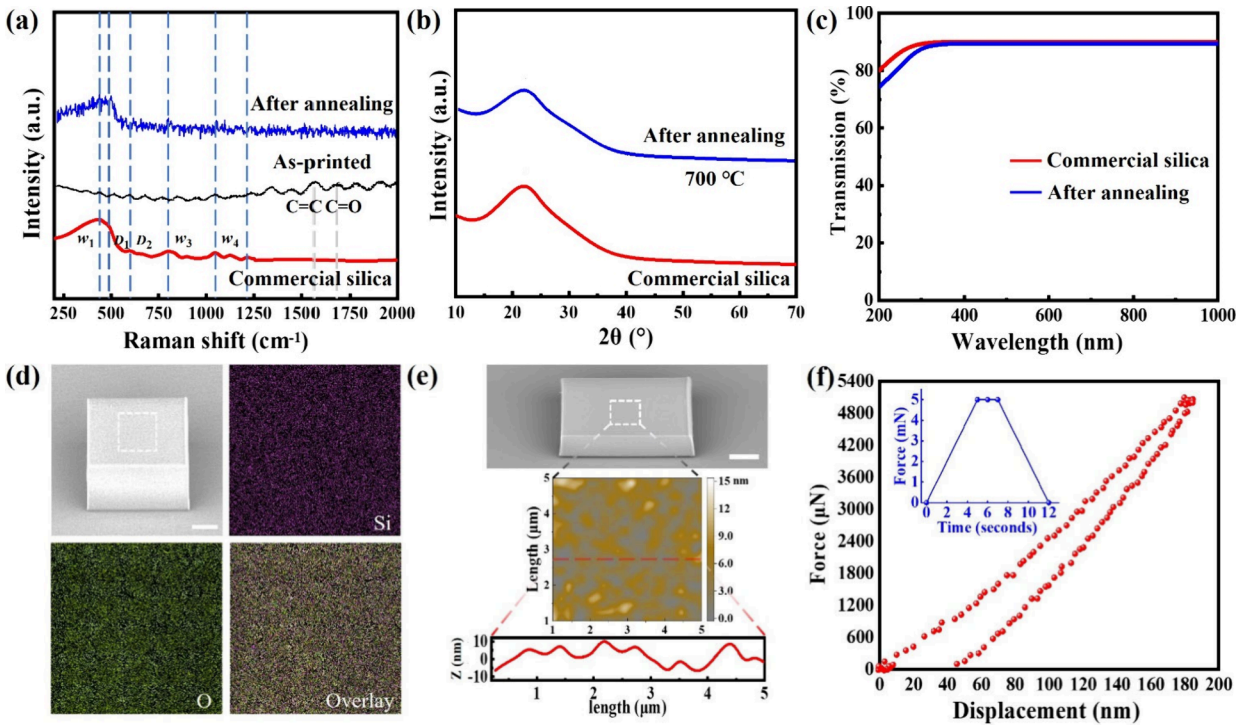

Figure 2. Material and structure characterizations of ultrafast laser-lithographed fiber-integrated silica glass. (a) Raman spectra of printed micro/nanostructures before and after thermal treatment. (b) XRD spectra of fabricated silica and commercial fused silica. (c) Normalized optical transmission spectra of fabricated silica and commercial fused silica. (d) EDS elemental mapping of fabricated silica cuboid. (e) AFM image of fabricated silica cuboid and the line profile of the top surface. (f) The measured applied force−displacement curve of the fabricated silica. Inset is the applied force−time curve. Scale bars: (d) 10 μm and (e) 5 μm.

conversion of the liquid resin into a solid structure.[38,39] The 3D structures were fabricated by moving the laser beam by using galvanometer mirrors for in-plane scanning and adjusting the position of the sample stage along three axes. Following the laser printing, an isopropyl alcohol bath, lasting for 4 min, effectively dissolved residual uncured resin. Subsequently, a moderate thermal treatment at 700 °C in an air environment transformed the initially printed structures into silica glass, benefiting from the densely packed continuous silicon−oxygen molecular networks. The applied temperature caused the decomposition and release of organic compounds, and atmospheric oxygen facilitated the removal of the remaining carbon. A variety of 3D silica micro/nanostructures with high resolution and structural quality were manufactured, including a smooth aspherical microlenses array (Figure 1b,c), rectangular pyramid array (Figure 1d,e), single-layer woodpile micro/nanostructure array (Figure 1f,g), and complex multi-layer woodpile structures (Figure 1h,i) with an overall size of 32 μm, containing individual bars with nanoscale details. Overall, fiber-integrated silica glass with a high structural quality and size scale can be fabricated through ultrafast laser multiphoton 3D nanolithography followed by low-temperature thermal treatment.

MORPHOLOGY AND STRUCTURE CHARACTERIZATIONS OF FIBER-INTEGRATED SILICA GLASS

To confirm that the printed acrylate-functionalized POSS without additional acrylic oligomers were converted to silica glass after annealing at 700 °C, the related material characterizations were conducted. Figure 2a shows the Raman spectra of the printed organic−inorganic structures before and after thermal treatment. For reference, the spectrum of commercial silica is provided. The w_1 and w_3 bands are attributed to the bending vibrations of Si−O−Si bridges, while the w_4 bands are associated with the stretching of Si−O bonds. The D_1 and D_2 bands correspond to the symmetric stretching of silicon−oxygen rings.[40] In contrast to the commercial silica signal, the spectrum of the as-printed structures exhibited characteristics typical of a thermoset material. In this spectrum, the most prominent peaks were associated with the C═C and C═O bonds.[41] After heat treatment, the organic peaks were entirely absent, and the spectra of the fabricated structures and commercial silica were indistinguishable, suggesting that the printed organic−inorganic structures were transferred to silica after annealing at 700 °C. Figure 2b shows X-ray diffraction (XRD) results of printed structures after thermal treatment and commercial silica with a broad spectrum. This demonstrates that amorphous silica without crystalline phases was obtained. UV−visible (UV−vis) microspectrophotometry (Figure 2c) was conducted on a 20 μm-thick fabricated silica. Throughout the measurement range, there were no absorption bands, which demonstrates that the fabricated silica exhibited good optical properties comparable to those of commercial silica. Energy dispersive X-ray spectroscopy (EDS) mapping (Figure 2d) of the fabricated silica reveals a uniform distribution of silicon and oxygen without any observable aggregation. Upon excluding the negligible carbon content, the atomic percentages of silicon and oxygen were determined to be 34.3% and 65.7%, respectively, demonstrating nearly complete conversion into fused silica. The fabricated silica also exhibited a smooth surface and an exceptional mechanical strength. Atomic force microscopy (AFM) on a flat silica cuboid yielded a roughness of 4.5 nm (Figure 2e). When

https://doi.org/10.1021/acs.nanolett.4c02680
Nano Lett. 2024, 24, 9734−9742

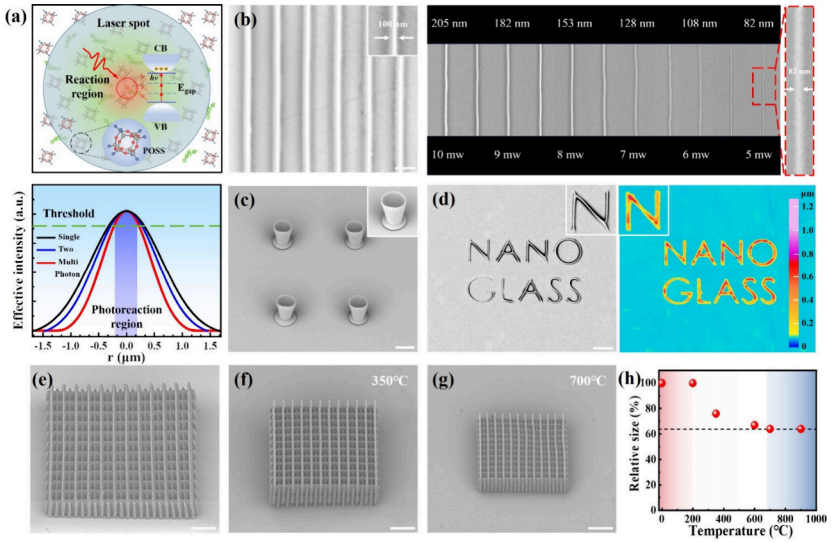

Figure 3. Formation process of ultrafast laser-fabricated fiber-integrated silica glass by multiphoton 3D nanolithography. (a) Illustration of printed POSS with subdiffraction resolution by an ultrafast laser-induced nonlinear effect. The blue circle denotes the laser focus spot. The inset displays the molecular structure of POSS. The dashed green line represents the polymerization threshold. (b) SEM image of silica nanowires manufactured by multiphoton lithography with various laser powers. Inset is the silica nanowire with the narrowest line width of 82 nm. (c) SEM image of silica goblet array. The inset displays the zoomed-in view of the goblet array. (d) SEM and white light interferometer images of the letters "NANO GLASS". The inset displays the zoomed-in top view of the letter "N". (e) Tilt-view SEM image of the printed double-layer woodpile structure before heat treatment. Tilt-view SEM image of the printed double-layer woodpile structure calcinated at (f) 350 and (g) 700 °C. (h) Measured sizes of as-printed woodpile under thermal treatment with increasing temperature. Scale bars: (b) 200 nm, (c) 20 μm, and (d, e, f, g) 10 μm.

subjected to compression testing, the silica cuboid showed a hardness of 7.1 GPa (Figure 2f). The measured Young's modulus, which reached up to 58 GPa, was within the range of dense silica.[42]

FORMATION PROCESS OF ULTRAFAST LASER-FABRICATED FIBER-INTEGRATED SILICA GLASS

The ultrafast laser 3D nanolithography of fiber-integrated silica glass with nanoscale resolution was demonstrated based on the threshold effect, which exists in the nonlinear photoreaction.[43,44] It exhibits a highly nonlinear dependence on the femtosecond laser fluence as the intensity approaches the threshold. The effective intensity profile becomes increasingly narrow as the number of simultaneously absorbed photons rises (Figure 3a). Careful control of the laser fluence allows for creating structure features beyond the optical diffraction limit by ensuring that only a fraction of the focal spot surpasses the polymerization threshold. The setup is more efficient in terms of radiation intensity than the one used by TPP,[26] and therefore, it is sufficient for triggering enough cross-linking in the pure POSS to generate a stable structure in the green state. Figure 3b shows an SEM image of silica nanowires manufactured by multiphoton lithography and subsequent heat treatment. Parallel nanowires featuring 100 nm in line width and a 350 nm periodicity have been realized. This small periodicity of 350 nm makes these nanowires well-suited for producing high-performance optical devices. By precisely adjusting the laser fluence, an 82 nm silica nanowire was successfully fabricated, corresponding to $\lambda/12$ of the 1030 nm wavelength. This is comparable to the silica structures produced using the TPP strategy.[26] The nanowire exhibits well-defined edges and a smooth contour, implying the potential for achieving even smaller structures by approaching the threshold more closely. Numerous micro/nanostructures were fabricated to illustrate the potential for creating diverse features using ultrafast laser multiphoton nanolithography, including silica cuboid and cylinder arrays (Figures S1 and S2), silica microcantilevers (Figure S3), a silica goblet array with smooth sidewalls (Figures 3c and S4), and the letters "NANO GLASS" with uniform line width and height (Figures 3d and S5). The formation process of the as-printed structures under thermal treatment with increasing temperature was further investigated (Figures 3e–g and S6). Following heat treatment, cross-linked acrylic-functional POSS may undergo thermo-oxidative degradation, involving peroxide group formation, random chain scission, and releasing compounds such as carbon dioxide, water, and hydrocarbons.[45,46] Due to the adsorption force of the substrate, the printed structures may undergo anisotropic shrinkage during the sintering process. This issue could be effectively addressed from a design level: printing a structure that appears distorted in the green state but becomes isotropic after firing according to differential shrinkage occurring within the structure. Dimensional analyses conducted at progressively elevated temperatures, ranging from the initial as-printed state to as high as 900 °C, revealed that the printed structures underwent a linear contraction of 36% during the thermal conversion process (Figure 3h). The printed structure maintained its precise geometric integrity even when subjected to high-temperature conditions. Remarkably, after reaching 700 °C, the fabricated silica exhibited high geometric stability, showing no noticeable further shrinkage (Figure S7). Correspondingly, the most intricate nanostructures withstood elevated temperatures without experiencing distortion or damage.

https://doi.org/10.1021/acs.nanolett.4c02680
Nano Lett. 2024, 24, 9734−9742

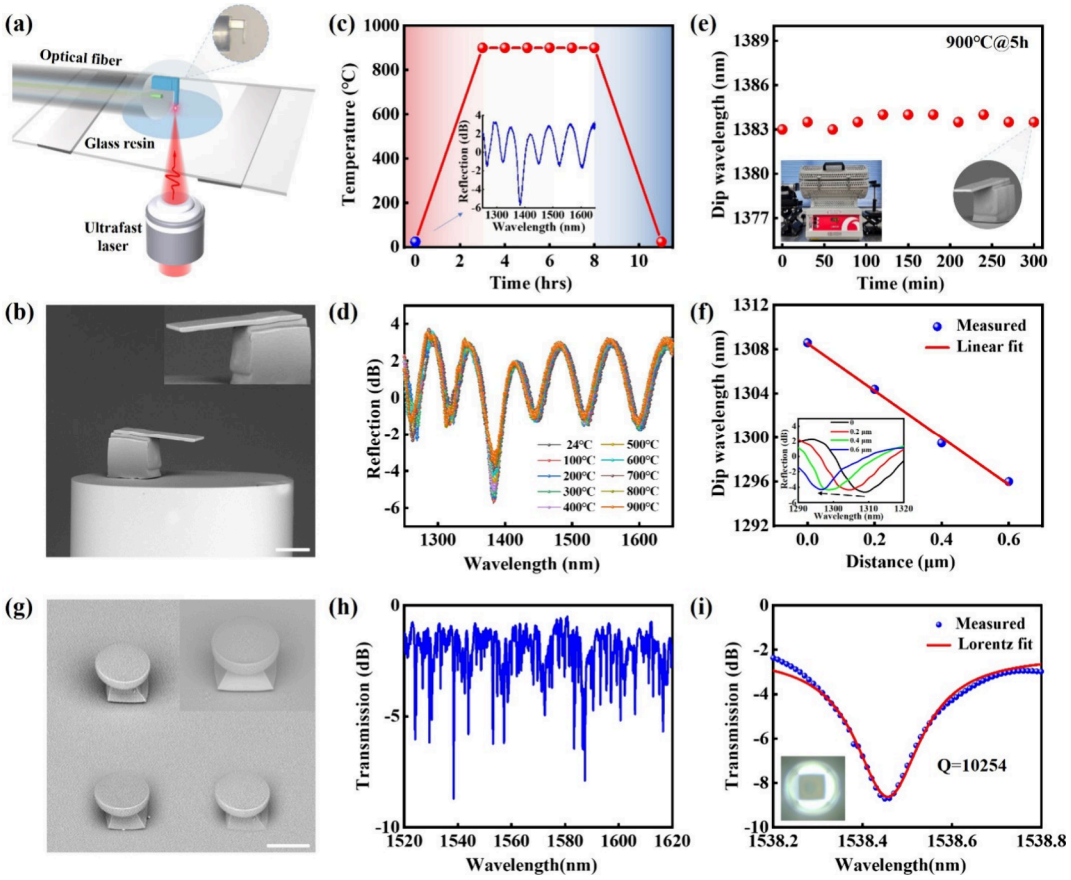

Figure 4. Optical properties of ultrafast laser multiphoton-lithographed fiber-integrated functional silica devices. (a) Schematic of the 3D printing of microcantilever probes on the optical fiber tip. (b) SEM image of the fabricated fiber-tip silica microcantilever probes. Inset is the zoomed-in view of the microcantilever. High-temperature stability of the fabricated fiber-tip microcantilever probes: (c) applied temperature−time profile (inset is the original reflection spectra of the fiber-tip microcantilever), (d) reflection spectra of the fiber-tip microcantilever under different temperatures, and (e) repeated measurements of the dip wavelength at 900 °C for 5 h (insets are the heating equipment and SEM image of microcantilever after 900 °C treatment for 5 h). (f) Linear fitting of the dip wavelength with respect to the applied displacement. Inset is the reflection spectra under various applied displacements. (g) SEM image of the fabricated microtoroid optical resonator. Inset is the zoomed-in view of the microtoroid. (h) Transmission spectrum of the fabricated microtoroid resonator. (i) Fitting of a quality factor at 1538.45 nm. Inset is the optical microscopy image of the microtoroid resonator. Scale bars: (b, g) 20 μm.

OPTICAL PROPERTIES OF ULTRAFAST LASER-FABRICATED FIBER-INTEGRATED FUNCTIONAL SILICA DEVICES

The strategy for ultrafast laser multiphoton 3D nanolithography followed by low-temperature heat treatment can be used to realize the direct integration of silica functional micro/nanostructures. To demonstrate the optical properties, silica microcantilever probes were fabricated on the optical fiber tip. Optical fibers have a softening point at 1000 °C, which makes the direct integration of silica micro/nanostructures impossible when using the traditional TPP strategy followed by high-temperature heat treatment. Figure 4a schematically illustrates the 3D printing of the microcantilever on the optical fiber tip with a 125 μm diameter.[1,2,47] As shown in Figure 4b, the silica microstructure consists of two components: a supporting base and a cantilever beam (Figure S8). The base stands at a height of approximately 25 μm, with a cross-sectional area measuring 25 × 20 μm^2 to ensure a reliable connection with the optical fiber tip. The upper section of the base was connected to a cantilever beam with a length of 50 μm, a width of 12 μm, and a thickness of 1.5 μm, which exhibited a smooth surface and a good parallelism. To investigate the high-temperature stability of the fabricated fiber-tip silica microcantilever probe, the optical fiber was placed in a tube furnace with an increase in temperature (Figure 4c). The reflection spectra of the silica cantilever at ambient temperature were measured using an amplified spontaneous emission light source and an optical spectrum analyzer (Figure S9). At approximately 1383 nm, measurements revealed a free spectral range of 60 nm and a fringe visibility of about 8 dB. The observed interference pattern can be comprehended as a result of three-beam interference, originating from the fiber tip, as well as the bottom and top facets of the cantilever.[48] When increasing the applied temperature from 24 to 900 °C, there was no change in the reflection spectra of the silica cantilever (Figure 4d). After heat treatment at 900 °C for 5 h, the dip wavelength of the spectrum also did not shift and the microcantilever maintained the intact structure, demonstrating the high-temperature stability of the fabricated functional structure. The fiber-tip silica microcantilever probe was used to investigate the external displacement response (Figures 4f and S10). The microcantilever probe on a piezo stage was gradually pressed toward a glass specimen in the step of 0.2 μm. The inset displays the changes in the reflection spectra of the microcantilever probe as the applied displacement increases from 0 to 0.6 μm. As

https://doi.org/10.1021/acs.nanolett.4c02680
Nano Lett. 2024, 24, 9734−9742

indicated by the arrow, a noticeable blue shift in the dip wavelength was observed. The dip wavelength against the applied displacement was plotted, and the displacement sensitivity of the microcantilever was calculated to be −17.5 nm μm^{-1}.

Whispering gallery resonators play a pivotal role in integrated photonics,[49−52] yet their manufacture is challenging due to inherently three-dimensional characteristics. Through multiphoton 3D nanolithography, we successfully fabricated a proof-of-concept microtoroid optical resonator, as shown in Figure 4g. In contrast to the commonly employed techniques involving photolithography and plasma etching to create a suspended disk and subsequently toroid formation through laser irradiation, the fabricated silica microtoroid optical resonator on a tapered base provides distinct advantages. The design of the supporting base can be optimized for an enhanced mechanical robustness. In addition, this method allows for precise control over the toroid morphology, a feature that is challenging to achieve, particularly when dealing with larger-diameter disks. Through precise control of the microtoroid morphology, optical resonators with diverse shapes have been manufactured and achieved high quality factors (Figure S11). Figure 4h shows the transmission spectrum and a standard resonance response of the fabricated microtoroid resonator. The quality factor achieves 1×10^4 at 1538 nm (Figure 4i).

This work represents a significant advancement in integrated optics, enabling the direct printing of silica microdevices with superior mechanical and optical properties onto fiber tips, which holds promise for applications in fiber sensing. Unlike printed polymers, the printed silica structure exhibits resistance to common chemicals, including organic solvents. The integration of a microcantilever with the fiber end face creates an open Fabry−Pérot interferometer capable of measuring the refractive index of organic solvents. Moreover, due to the good stability of the printed silica structures in harsh environments, high-temperature vibration sensing can be realized by integrating microcantilevers and proof masses on fiber tips. Finally, the potential of this approach could be further expanded by mixing other functional materials before printing, thereby tailoring the properties of the final structure. For example, introducing rare-earth elements would enable active photonic integration, while adding ferrous nanomaterials could facilitate magnetic field detection by using fiber-integrated silica microdevices.

In summary, we proposed a strategy for ultrafast laser multiphoton 3D nanolithography of fiber-integrated silica. The acrylate-functionalized POSS can be locally cross-linked through an ultrafast laser-induced nonlinear effect. Without silica nanoparticles and polymer additives, the as-printed micro/nanostructures were converted to silica glass after annealing at 700 °C. Compared to linear absorption, the high-quality silica with sub-100 nm resolution can be fabricated by multiphoton absorption. Owing to the low calcination temperature, the printed structures were directly integrated on the optical fiber. Fiber-integrated silica microcantilever probes and microtoroid resonators were constructed by ultrafast laser multiphoton 3D nanolithography, with strong thermal stability and quality factors of over 10^4. This work expands the knowledge of fiber-integrated inorganic micro/nanostructure fabrication and provides a strategy for designing functional silica devices for a wide range of applications.

■ ASSOCIATED CONTENT

Supporting Information

The Supporting Information is available free of charge at https://pubs.acs.org/doi/10.1021/acs.nanolett.4c02680.

Materials, synthesis, characterization methods, fabrication process, SEM analyses reflection spectra, transmission spectra, and comparison of the fabrication characteristics (PDF)

■ AUTHOR INFORMATION

Corresponding Author

Changrui Liao − *Shenzhen Key Laboratory of Ultrafast Laser Micro/Nano Manufacturing, Key Laboratory of Optoelectronic Devices and Systems of Ministry of Education/Guangdong Province, College of Physics and Optoelectronic Engineering and Shenzhen Key Laboratory of Photonic Devices and Sensing Systems for Internet of Things, Guangdong and Hong Kong Joint Research Centre for Optical Fibre Sensors, State Key Laboratory of Radio Frequency Heterogeneous Integration, Shenzhen University, Shenzhen 518060, China;* orcid.org/0000-0003-3669-5054; Email: cliao@szu.edu.cn

Authors

Dezhi Zhu − *Shenzhen Key Laboratory of Ultrafast Laser Micro/Nano Manufacturing, Key Laboratory of Optoelectronic Devices and Systems of Ministry of Education/Guangdong Province, College of Physics and Optoelectronic Engineering and Shenzhen Key Laboratory of Photonic Devices and Sensing Systems for Internet of Things, Guangdong and Hong Kong Joint Research Centre for Optical Fibre Sensors, State Key Laboratory of Radio Frequency Heterogeneous Integration, Shenzhen University, Shenzhen 518060, China; Guangdong Laboratory of Artificial Intelligence and Digital Economy (SZ), Shenzhen 518060, China*

Shangben Jiang − *Shenzhen Key Laboratory of Ultrafast Laser Micro/Nano Manufacturing, Key Laboratory of Optoelectronic Devices and Systems of Ministry of Education/Guangdong Province, College of Physics and Optoelectronic Engineering and Shenzhen Key Laboratory of Photonic Devices and Sensing Systems for Internet of Things, Guangdong and Hong Kong Joint Research Centre for Optical Fibre Sensors, State Key Laboratory of Radio Frequency Heterogeneous Integration, Shenzhen University, Shenzhen 518060, China*

Lei Xu − *School of Electronic and Communication Engineering, Shenzhen Polytechnic University, Shenzhen 518055, China*

Ying Wang − *Shenzhen Key Laboratory of Ultrafast Laser Micro/Nano Manufacturing, Key Laboratory of Optoelectronic Devices and Systems of Ministry of Education/Guangdong Province, College of Physics and Optoelectronic Engineering and Shenzhen Key Laboratory of Photonic Devices and Sensing Systems for Internet of Things, Guangdong and Hong Kong Joint Research Centre for Optical Fibre Sensors, State Key Laboratory of Radio Frequency Heterogeneous Integration, Shenzhen University, Shenzhen 518060, China;* orcid.org/0000-0001-8020-3622

Dejun Liu − *Shenzhen Key Laboratory of Ultrafast Laser Micro/Nano Manufacturing, Key Laboratory of Optoelectronic Devices and Systems of Ministry of Education/*

https://doi.org/10.1021/acs.nanolett.4c02680
Nano Lett. 2024, 24, 9734−9742

Guangdong Province, College of Physics and Optoelectronic Engineering and Shenzhen Key Laboratory of Photonic Devices and Sensing Systems for Internet of Things, Guangdong and Hong Kong Joint Research Centre for Optical Fibre Sensors, State Key Laboratory of Radio Frequency Heterogeneous Integration, Shenzhen University, Shenzhen 518060, China

Weijia Bao − *Shenzhen Key Laboratory of Ultrafast Laser Micro/Nano Manufacturing, Key Laboratory of Optoelectronic Devices and Systems of Ministry of Education/ Guangdong Province, College of Physics and Optoelectronic Engineering and Shenzhen Key Laboratory of Photonic Devices and Sensing Systems for Internet of Things, Guangdong and Hong Kong Joint Research Centre for Optical Fibre Sensors, State Key Laboratory of Radio Frequency Heterogeneous Integration, Shenzhen University, Shenzhen 518060, China*

Famei Wang − *Shenzhen Key Laboratory of Ultrafast Laser Micro/Nano Manufacturing, Key Laboratory of Optoelectronic Devices and Systems of Ministry of Education/ Guangdong Province, College of Physics and Optoelectronic Engineering and Shenzhen Key Laboratory of Photonic Devices and Sensing Systems for Internet of Things, Guangdong and Hong Kong Joint Research Centre for Optical Fibre Sensors, State Key Laboratory of Radio Frequency Heterogeneous Integration, Shenzhen University, Shenzhen 518060, China*

Haoqiang Huang − *Shenzhen Key Laboratory of Ultrafast Laser Micro/Nano Manufacturing, Key Laboratory of Optoelectronic Devices and Systems of Ministry of Education/ Guangdong Province, College of Physics and Optoelectronic Engineering and Shenzhen Key Laboratory of Photonic Devices and Sensing Systems for Internet of Things, Guangdong and Hong Kong Joint Research Centre for Optical Fibre Sensors, State Key Laboratory of Radio Frequency Heterogeneous Integration, Shenzhen University, Shenzhen 518060, China*

Xiaoyu Weng − *Shenzhen Key Laboratory of Ultrafast Laser Micro/Nano Manufacturing, Key Laboratory of Optoelectronic Devices and Systems of Ministry of Education/ Guangdong Province, College of Physics and Optoelectronic Engineering, Shenzhen University, Shenzhen 518060, China*

Liwei Liu − *Shenzhen Key Laboratory of Ultrafast Laser Micro/Nano Manufacturing, Key Laboratory of Optoelectronic Devices and Systems of Ministry of Education/ Guangdong Province, College of Physics and Optoelectronic Engineering, Shenzhen University, Shenzhen 518060, China;* orcid.org/0000-0002-4593-665X

Junle Qu − *Shenzhen Key Laboratory of Ultrafast Laser Micro/Nano Manufacturing, Key Laboratory of Optoelectronic Devices and Systems of Ministry of Education/ Guangdong Province, College of Physics and Optoelectronic Engineering, Shenzhen University, Shenzhen 518060, China*

Yiping Wang − *Shenzhen Key Laboratory of Ultrafast Laser Micro/Nano Manufacturing, Key Laboratory of Optoelectronic Devices and Systems of Ministry of Education/ Guangdong Province, College of Physics and Optoelectronic Engineering and Shenzhen Key Laboratory of Photonic Devices and Sensing Systems for Internet of Things, Guangdong and Hong Kong Joint Research Centre for Optical Fibre Sensors, State Key Laboratory of Radio Frequency Heterogeneous Integration, Shenzhen University, Shenzhen 518060, China; Guangdong Laboratory of Artificial Intelligence and Digital Economy (SZ), Shenzhen 518060, China*

Complete contact information is available at: https://pubs.acs.org/10.1021/acs.nanolett.4c02680

Author Contributions

[▽]D.Z. and S.J. contributed equally to this work. C.L. and Y.W. (Yiping Wang) conceived the idea. D.Z., S.J., L.X., Y.W. (Ying Wang), D.L., and W.B. contributed to the experimental investigation. F.W. and H.H. analyzed the data. D.Z., S.J., C.L., and Y.W. (Yiping Wang) wrote the manuscript, and all authors contributed to editing the final manuscript.

Notes

The authors declare no competing financial interest.

■ ACKNOWLEDGMENTS

This work was supported by the Shenzhen Science and Technology Program (RCYX20200714114524139, Shenzhen Key Laboratory of Ultrafast Laser Micro/Nano Manufacturing ZDSYS20220606100405013), Natural Science Foundation of Guangdong Province (2022B1515120061), National Natural Science Foundation of China (62122057, 62075136), Postdoctoral Fellowship Program of China Postdoctoral Science Foundation (GZC20231722), Research Team Cultivation Program of Shenzhen University (2023QNT009), and Medicine Plus Program of Shenzhen University (2024YG013).

■ REFERENCES

(1) Zou, M.; Liao, C.; Liu, S.; Xiong, C.; Zhao, C.; Zhao, J.; Gan, Z.; Chen, Y.; Yang, K.; Liu, D.; Wang, Y.; Wang, Y. Fiber-tip polymer clamped-beam probe for high-sensitivity nanoforce measurements. *Light: Science & Applications* **2021**, *10*, 171.

(2) Liao, C.; Xiong, C.; Zhao, J.; Zou, M.; Zhao, Y.; Li, B.; Ji, P.; Cai, Z.; Gan, Z.; Wang, Y.; Wang, Y. Design and realization of 3D printed fiber-tip microcantilever probes applied to hydrogen sensing. *Light: Advanced Manufacturing* **2022**, *3*, 5.

(3) Shang, X.; Wang, N.; Cao, S.; Chen, H.; Fan, D.; Zhou, N.; Qiu, M. Fiber-Integrated Force Sensor using 3D Printed Spring-Composed Fabry-Perot Cavities with a High Precision Down to Tens of Piconewton. *Adv. Mater.* **2024**, *36*, No. 2305121.

(4) Li, F.; Liu, S.-F.; Liu, W.; Hou, Z.-W.; Jiang, J.; Fu, Z.; Wang, S.; Si, Y.; Lu, S.; Zhou, H.; et al. 3D printing of inorganic nanomaterials by photochemically bonding colloidal nanocrystals. *Science* **2023**, *381*, 1468−1474.

(5) Liu, S.-F.; Hou, Z.-W.; Lin, L.; Li, F.; Zhao, Y.; Li, X.-Z.; Zhang, H.; Fang, H.-H.; Li, Z.; Sun, H.-B. 3D nanoprinting of semiconductor quantum dots by photoexcitation-induced chemical bonding. *Science* **2022**, *377*, 1112−1116.

(6) Sun, K.; Tan, D.; Fang, X.; Xia, X.; Lin, D.; Song, J.; Lin, Y.; Liu, Z.; Gu, M.; Yue, Y.; Qiu, J. Three-dimensional direct lithography of stable perovskite nanocrystals in glass. *Science* **2022**, *375*, 307−310.

(7) Han, F.; Gu, S.; Klimas, A.; Zhao, N.; Zhao, Y.; Chen, S.-C. Three-dimensional nanofabrication via ultrafast laser patterning and kinetically regulated material assembly. *Science.* **2022**, *378*, 1325−1331.

(8) Wang, Y.; Fedin, I.; Zhang, H.; Talapin, D. V. Direct optical lithography of functional inorganic nanomaterials. *Science.* **2017**, *357*, 385−388.

(9) Zhang, D.; Xiao, W.; Liu, C.; Liu, X.; Ren, J.; Xu, B.; Qiu, J. Highly efficient phosphor-glass composites by pressureless sintering. *Nat. Commun.* **2020**, *11*, 2805.

(10) Kotz, F.; Risch, P.; Arnold, K.; Sevim, S.; Puigmarti-Luis, J.; Quick, A.; Thiel, M.; Hrynevich, A.; Dalton, P. D.; Helmer, D.; Rapp, B. E. Fabrication of arbitrary three-dimensional suspended hollow

microstructures in transparent fused silica glass. *Nat. Commun.* **2019**, *10*, 1439.
(11) Papadopoulos, A.; Skoulas, E.; Mimidis, A.; Perrakis, G.; Kenanakis, G.; Tsibidis, G. D.; Stratakis, E. Biomimetic omnidirectional antireflective glass via direct ultrafast laser nanostructuring. *Adv. Mater.* **2019**, *31*, No. 1901123.
(12) Sakr, H.; Chen, Y.; Jasion, G. T.; Bradley, T. D.; Hayes, J. R.; Mulvad, H. C. H.; Davidson, I. A.; Numkam Fokoua, E.; Poletti, F. Hollow core optical fibres with comparable attenuation to silica fibres between 600 and 1100 nm. *Nat. Commun.* **2020**, *11*, 6030.
(13) Croissant, J. G.; Butler, K. S.; Zink, J. I.; Brinker, C. J. Synthetic amorphous silica nanoparticles: toxicity, biomedical and environmental implications. *Nature Reviews Materials* **2020**, *5*, 886−909.
(14) Kotz, F.; Arnold, K.; Bauer, W.; Schild, D.; Keller, N.; Sachsenheimer, K.; Nargang, T. M.; Richter, C.; Helmer, D.; Rapp, B. E. Three-dimensional printing of transparent fused silica glass. *Nature* **2017**, *544*, 337−339.
(15) Toombs, J. T.; Luitz, M.; Cook, C. C.; Jenne, S.; Li, C. C.; Rapp, B. E.; Kotz-Helmer, F.; Taylor, H. K. Volumetric additive manufacturing of silica glass with microscale computed axial lithography. *Science* **2022**, *376*, 308−312.
(16) Moore, D. G.; Barbera, L.; Masania, K.; Studart, A. R. Three-dimensional printing of multicomponent glasses using phase-separating resins. *Nat. Mater.* **2020**, *19*, 212−217.
(17) Kotz, F.; Quick, A. S.; Risch, P.; Martin, T.; Hoose, T.; Thiel, M.; Helmer, D.; Rapp, B. E. Two-photon polymerization of nanocomposites for the fabrication of transparent fused silica glass microstructures. *Adv. Mater.* **2021**, *33*, No. 2006341.
(18) Wen, X.; Zhang, B.; Wang, W.; Ye, F.; Yue, S.; Guo, H.; Gao, G.; Zhao, Y.; Fang, Q.; Nguyen, C.; Zhang, X.; Bao, J.; Robinson, J. T.; Ajayan, P. M.; Lou, J. 3D-printed silica with nanoscale resolution. *Nat. Mater.* **2021**, *20*, 1506−1511.
(19) Li, M.; Yue, L.; Rajan, A. C.; Yu, L.; Sahu, H.; Montgomery, S. M.; Ramprasad, R.; Qi, H. J. Low-temperature 3D printing of transparent silica glass microstructures. *Sci. Adv.* **2023**, *9*, eadi2958.
(20) Hong, Z.; Ye, P.; Loy, D. A.; Liang, R. Three-dimensional printing of glass micro-optics. *Optica.* **2021**, *8*, 904−910.
(21) Bauer, J.; Schroer, A.; Schwaiger, R.; Kraft, O. Approaching theoretical strength in glassy carbon nanolattices. *Nat. Mater.* **2016**, *15*, 438−443.
(22) Gonzalez-Hernandez, D.; Varapnickas, S.; Merkininkaitė, G.; Čiburys, A.; Gailevičius, D.; Šakirzanovas, S.; Juodkazis, S.; Malinauskas, M. Laser 3D Printing of Inorganic Free-Form Micro-Optics. *Photonics* **2021**, *8*, 577.
(23) Huang, P.-H.; Laakso, M.; Edinger, P.; Hartwig, O.; Duesberg, G. S.; Lai, L.-L.; Mayer, J.; Nyman, J.; Errando-Herranz, C.; Stemme, G.; Gylfason, K. B.; Niklaus, F. Three-dimensional printing of silica glass with sub-micrometer resolution. *Nat. Commun.* **2023**, *14*, 3305.
(24) Jin, F.; Liu, J.; Zhao, Y.-Y.; Dong, X.-Z.; Zheng, M.-L.; Duan, X.-M. $\lambda/30$ inorganic features achieved by multi-photon 3D lithography. *Nat. Commun.* **2022**, *13*, 1357.
(25) Lai, L.-L.; Huang, P.-H.; Stemme, G. r.; Niklaus, F.; Gylfason, K. B. 3D Printing of Glass Micro-Optics with Subwavelength Features on Optical Fiber Tips. *ACS Nano* **2024**, *18*, 10788−10797.
(26) Bauer, J.; Crook, C.; Baldacchini, T. A sinterless, low-temperature route to 3D print nanoscale optical-grade glass. *Science* **2023**, *380*, 960−966.
(27) Colombo, P.; Franchin, G. Improving glass nanostructure fabrication. *Science* **2023**, *380*, 895−896.
(28) Zhou, D.-L.; Li, J.-H.; Guo, Q.-Y.; Lin, X.; Zhang, Q.; Chen, F.; Han, D.; Fu, Q. Polyhedral oligomeric silsesquioxanes based ultralow-k materials: the effect of cage size. *Adv. Funct. Mater.* **2021**, *31*, No. 2102074.
(29) Fang, G.; Cao, H.; Cao, L.; Duan, X. Femtosecond Laser Direct Writing of 3D Silica-like Microstructure from Hybrid Epoxy Cyclohexyl POSS. *Advanced Materials Technologies* **2018**, *3*, No. 1700271.
(30) Yu, Y.; Prudnikau, A.; Lesnyak, V.; Kirchner, R. Quantum Dots Facilitate 3D Two-Photon Laser Lithography. *Adv. Mater.* **2023**, *35*, No. 2211702.
(31) Wang, H.; Zhang, W.; Ladika, D.; Yu, H.; Gailevicius, D.; Wang, H.; Pan, C.-F.; Nair, P. N. S.; Ke, Y.; Mori, T.; Chan, J. Y. E.; Ruan, Q.; Farsari, M.; Malinauskas, M.; Juodkazis, S.; Gu, M.; Yang, J. K. W. Two-Photon Polymerization Lithography for Optics and Photonics: Fundamentals, Materials, Technologies, and Applications. *Adv. Funct. Mater.* **2023**, *33*, No. 2214211.
(32) Gan, Z.; Cao, Y.; Evans, R. A.; Gu, M. Three-dimensional deep sub-diffraction optical beam lithography with 9 nm feature size. *Nat. Commun.* **2013**, *4*, 2061.
(33) Liaros, N.; Fourkas, J. T. Methods for determining the effective order of absorption in radical multiphoton photoresists: a critical analysis. *Laser & Photonics Reviews* **2021**, *15*, No. 2000203.
(34) Zhu, D.; Xie, J.; Yan, J.; He, G.; Qiao, M. Ultrafast laser plasmonic fabrication of nanocrystals by molecule modulation for photoresponse multifunctional structures. *Adv. Mater.* **2023**, *35*, No. 2211983.
(35) Zhang, J.; Zhu, D.; Yan, J.; Wang, C.-A. Strong metal-support interactions induced by an ultrafast laser. *Nat. Commun.* **2021**, *12*, 6665.
(36) Zhu, D.; Yan, J.; Xie, J.; Liang, Z.; Bai, H. Ultrafast laser-induced atomic structure transformation of Au nanoparticles with improved surface activity. *ACS Nano* **2021**, *15*, 13140−13147.
(37) Zhu, D.; Qiao, M.; Yan, J.; Xie, J.; Guo, H.; Deng, S.; He, G.; Zhao, Y.; Luo, M. Three-dimensional patterning of MoS2 with ultrafast laser. *Nanoscale.* **2023**, *15*, 14837−14846.
(38) Liu, S.-F.; Hou, Z.-W.; Lin, L.; Li, Z.; Sun, H.-B. 3D Laser Nanoprinting of Functional Materials. *Adv. Funct. Mater.* **2023**, *33*, No. 2211280.
(39) Ouyang, W.; Xu, X.; Lu, W.; Zhao, N.; Han, F.; Chen, S.-C. Ultrafast 3D nanofabrication via digital holography. *Nat. Commun.* **2023**, *14*, 1716.
(40) Zhang, H.; Li, F.; Song, H.; Liu, Y.; Huang, L.; Zhao, S.; Xiong, Z.; Wang, Z.; Dong, Y.; Liu, H. Random Silica-Glass Microlens Arrays Based on the Molding Technology of Photocurable Nanocomposites. *ACS Appl. Mater. Interfaces* **2023**, *15*, 19230−19240.
(41) Bauer, J.; Guell Izard, A.; Zhang, Y.; Baldacchini, T.; Valdevit, L. Programmable mechanical properties of two-photon polymerized materials: from nanowires to bulk. *Advanced Materials Technologies* **2019**, *4*, No. 1900146.
(42) Bruns, S.; Johanns, K. E.; Rehman, H. U.; Pharr, G. M.; Durst, K. Constitutive modeling of indentation cracking in fused silica. *J. Am. Ceram. Soc.* **2017**, *100*, 1928−1940.
(43) Kawata, S.; Sun, H.-B.; Tanaka, T.; Takada, K. Finer features for functional microdevices. *Nature.* **2001**, *412*, 697−698.
(44) Liu, K.; Ding, H.; Li, S.; Niu, Y.; Zeng, Y.; Zhang, J.; Du, X.; Gu, Z. 3D printing colloidal crystal microstructures via sacrificial-scaffold-mediated two-photon lithography. *Nat. Commun.* **2022**, *13*, 4563.
(45) Li, L.; Liang, R.; Li, Y.; Liu, H.; Feng, S. Hybrid thiol−ene network nanocomposites based on multi (meth) acrylate POSS. *J. Colloid Interface Sci.* **2013**, *406*, 30−36.
(46) Krongauz, V. V. Crosslink density dependence of polymer degradation kinetics: photocrosslinked acrylates. *Thermochim. Acta* **2010**, *503*, 70−84.
(47) Zou, M.; Liao, C.; Chen, Y.; Xu, L.; Tang, S.; Xu, G.; Ma, K.; Zhou, J.; Cai, Z.; Li, B.; Zhao, C.; Xu, Z.; Shen, Y.; Liu, S.; Wang, Y.; Gan, Z.; Wang, H.; Zhang, X.; Kasas, S.; Wang, Y. 3D printed fiber-optic nanomechanical bioprobe. *International Journal of Extreme Manufacturing* **2023**, *5*, No. 015005.
(48) Huang, H.; Liao, C.; Zou, M.; Liu, D.; Liu, S.; Wang, Y.; Bai, Z.; Liu, D.; Li, B.; Huang, J.; Wang, F.; Zhou, J.; Zhao, C.; Weng, X.; Liu, L.; Qu, J.; Wang, Y. Four-Dimensional Printing of a Fiber-Tip Multimaterial Microcantilever as a Magnetic Field Sensor. *ACS Photonics* **2023**, *10*, 1916.
(49) Jiang, X.; Yang, L. Optothermal dynamics in whispering-gallery microresonators. *Light: Science & Applications* **2020**, *9*, 24.

https://doi.org/10.1021/acs.nanolett.4c02680
Nano Lett. 2024, 24, 9734−9742

(50) Yu, D.; Humar, M.; Meserve, K.; Bailey, R. C.; Chormaic, S. N.; Vollmer, F. Whispering-gallery-mode sensors for biological and physical sensing. *Nature reviews methods primers* **2021**, *1*, 83.
(51) Kim, K.; Yoon, S.; Seo, M.; Lee, S.; Cho, H.; Meyyappan, M.; Baek, C.-K. Whispering gallery modes enhance the near-infrared photoresponse of hourglass-shaped silicon nanowire photodiodes. *Nature Electronics* **2019**, *2*, 572−579.
(52) Kfir, O.; Lourenço-Martins, H.; Storeck, G.; Sivis, M.; Harvey, T. R.; Kippenberg, T. J.; Feist, A.; Ropers, C. Controlling free electrons with optical whispering-gallery modes. *Nature* **2020**, *582*, 46−49.

https://doi.org/10.1021/acs.nanolett.4c02680
Nano Lett. 2024, 24, 9734−9742